Acta Crystallographica Section B
Structural Science
ISSN 0108-7681

Ab initio determination of the valence electron distribution in the average structure of the incommensurately modulated calaverite $AuTe_2$

Razvan Caracas* and Xavier Gonze

Université Catholique de Louvain, Laboratoire de Physico-Chimie et de Physique de Matériaux, pl. Croix du Sud 1, 1348 Louvain-la-Neuve, Belgium

Correspondence e-mail: caracas@pcpm.ucl.ac.be

Received 3 October 2000
Accepted 9 July 2001

The valence-electron density distribution of the average structure of incommensurately modulated calaverite, $AuTe_2$, has been computed using density-functional theory. High-density regions, centered around the Au and Te atoms, are not spheric, but present charge concentrations along the Au—Te and Te—Te bonds. The electronic band structure and its corresponding density of states reveal the presence of three electronic band groups, constituted mainly by Te 5*s*, Au 5*d* and hybrids of Te 6*p* + Au 6*s* + Au 5*d* orbitals. The electrons belonging to the last block are responsible for the chemical bonds.

1. Introduction

Calaverite is one of the best known examples of incommensurately modulated structures. The first attempts to index its morphology using rational indices failed at the beginning of the century (Smith, 1902; Goldschmidt *et al.*, 1931). More recent studies (Dam *et al.*, 1985; Janner & Dam, 1989) solved the face-indexation problem by describing the morphology and the crystal symmetry in a four-dimensional space, with a monoclinic average structure and a modulation wavevector $\mathbf{q} = -0.41\mathbf{a}^* + 0.45\mathbf{c}^*$. Independently, Schutte & de Boer (1988) performed an X-ray refinement of the calaverite structure in four-dimensional space and found a *C*2/*m* average structure with a modulation wavevector $\mathbf{q} = -0.4076\ \mathbf{a}^* + 0.4479\ \mathbf{c}^*$, in agreement with the face-indexation solution.

In the average structure, each Au atom has two apical and four equatorial Te neighbors, the equatorial ones being slightly more distant than the apical ones. Owing to the modulations, the equatorial set of Te atoms is displaced with respect to the centered Au atom: two Te atoms come closer to it. This fact was interpreted by Schutte & de Boer (1988) as a valence fluctuation of Au in the structure. Later X-ray photoelectron spectroscopy measurements showed a single valence state for Au (van Triest *et al.*, 1990).

In order to clarify electronic and chemical properties of the average structure we determined the valence-electron density distribution using the density-functional theory (DFT hereafter) formalism (Hohenberg & Kohn, 1964; Kohn & Sham, 1965). It is an established fact that the electron density distribution determined by *ab initio* approaches such as

Hartree–Fock calculations (Causa *et al.*, 1986) or DFT (Charlier *et al.*, 1991) fall within the experimental error bar of X-ray determinations. In a complementary study of the average structure of calaverite (Gonze *et al.*, 2001) we determined the equilibrium geometry within the DFT.

In §2 we present the *ab initio* parameters involved in the calculation and the average structure. In §3 we present the total valence-electron density distribution and its decomposition into electronic bands with the assigned orbitals. We will also discuss some physical and chemical bonding aspects in relation to the electron distribution.

2. Computational details

Throughout this study we considered the average monoclinic structure determined at 100 K (Schutte & de Boer, 1988): unit-cell parameters $a_0 = 7.182$, $b_0 = 4.402$ Å and $c_0 = 5.056$ Å, with $\beta = 89.99°$. The Au atoms are in the 2(*a*) Wyckoff positions (0,0,0) and the Te atoms in the 4(*i*) Wyckoff positions (x,0,z), with $x = 0.6890$ and $z = 0.2888$ (Schutte & de Boer, 1988). The Au has coordination 6: there are two short apical Au—Te bonds of 2.6680 Å and four long equatorial Au—Te bonds of 2.9698 Å forming a distorted octahedron. This structure is stable for pressures up to 2.50 GPa (Reithmayer *et al.*, 1993).

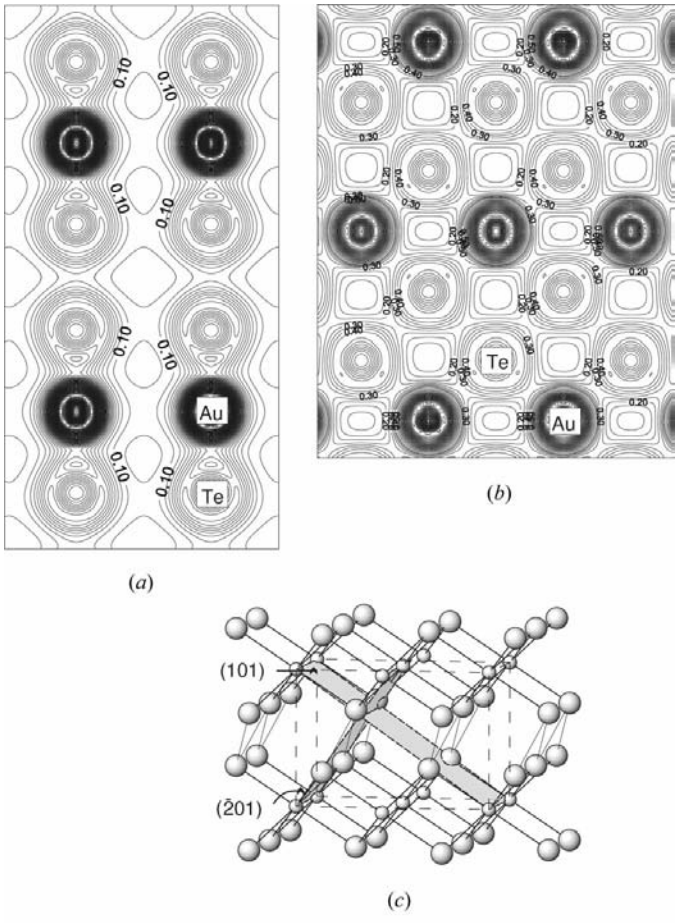

Figure 1
Total valence electron density in (*a*) the (101) and (*b*) the (2̄01) plane of the average structure of calaverite. The contours interval is 0.05 e Å^{-3}. The disposition of the two planes in the calaverite structure is represented schematically in (*c*).

All the calculations were based on the local density approximation (LDA) of the DFT (Hohenberg & Kohn, 1964; Kohn & Sham, 1965). We used the *ABINIT* code, a common project of the Université Catholique de Louvain, Corning Incorporated and other contributors (*ABINIT*v2.0, 1999; Gonze *et al.*, 2001). The *ABINIT* software is based on pseudopotentials and planewaves. It relies on the adaptation to a fixed potential of the band-by-band conjugate gradient method (Payne *et al.*, 1992) and on a potential-based conjugate-gradient algorithm for the determination of the self-consistent potential (Gonze, 1996). As usual with planewave basis sets, the numerical accuracy of the calculation can be systematically improved by increasing the cut-off kinetic energy of the planewaves. For example, it is free of the spherical shape approximation used in a previous electronic structure study of calaverite (Krutzen & Inglesfield, 1990).

The electronic properties (band structure and density of states) are obtained in the first Brillouin zone, using a regular $4 \times 4 \times 4$ grid of special k points (Monkhorst & Pack, 1976) with 16 points in the irreducible part of the Brillouin zone, and a planewave kinetic energy cut-off of 20 Hartree (1 Hartree = 27.211 eV). Within the pseudopotential-planewave approach the 'pseudo'-wavefunctions describe only the valence and conduction electrons, while the core electrons are taken into account using pseudopotentials. Moreover, the 'pseudo'-valence electron density coincides with the all-electron valence electron density outside the core region, but is smoothed inside it. We used Troullier–Martins pseudopotentials (Troullier & Martins, 1992) for both elements, the core electron configuration of Au being [Xe]$4f^{14}$ and that of Te being [Kr]$4d^{10}$.

After calculating self-consistently the total valence electron density distribution, we performed its decomposition in terms of contributions of the different orbitals. This allows us to assign a chemical significance to the electronic bands, identifying the corresponding orbitals and hybridization.

3. Results and discussion

Fig. 1 shows the total valence-electron density distribution in two planes through the apical (Fig. 1*a*) and the equatorial (Fig. 1*b*) planes of the $AuTe_6$ octahedron. In the equatorial (201) planes (Fig. 1*b*) containing Au and Te atoms, one finds the largest density regions. These high-density parallel planes are connected by Te–Au–Te–Te–Au–Te chains along [101] directions, seen in Fig. 1(*a*). In the same figure, one observes regions of low density, corresponding to chains of octahedral void spaces where the electron density presents a relatively flat distribution, with the density of the order 0.02–0.07 e Å^{-3}.

The 46 valence electrons of calaverite per conventional unit cell give an average valence electron density of 0.2877 e Å^{-3}. The areas of maximum electron concentration are found around the Au and Te atoms. By neglecting the core electrons, the local valence electron maxima are not located right on the atoms, but displaced by 0.5–0.6 Å and by 0.5–1 Å for the local

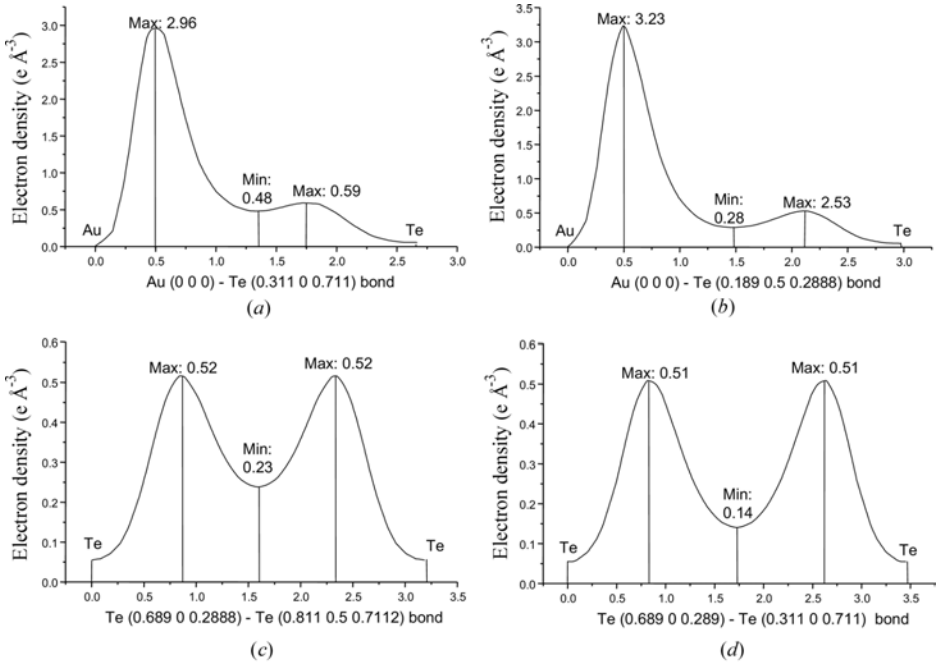

Figure 2
Total valence electron density along the Au—Te and Te—Te bonds in the average structure of calaverite (*a*) Au—Te apical bond; (*b*) Au—Te equatorial bond; (*c*) Te—Te bond within the $(\bar{2}01)$ plane; (*d*) Te—Te bond along $[\bar{1}01]$.

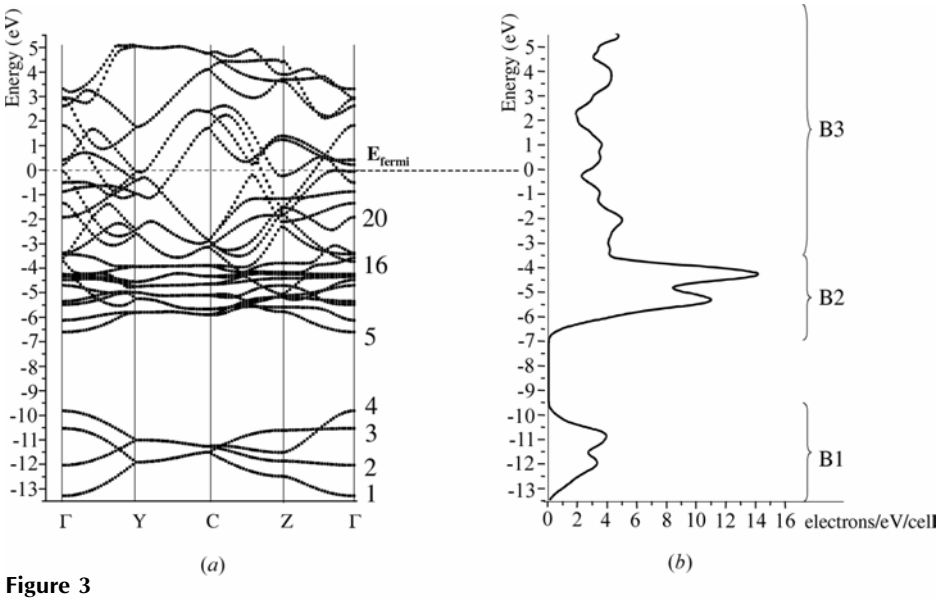

Figure 3
(*a*) Electronic band spectrum and (*b*) the density of states of the average structure of calaverite. The ΓYCZΓ path is along the edges of the Brillouin zone. Some selected electronic bands are numbered. The structure possesses metallic character. We can further separate three blocks of electronic bands: B1, containing the four bands which are the lowest in energy, B2, containing the next 12 electronic bands, and B3, comprising the rest of the electronic bands. Between the blocks B1 and B2 there is an energy gap of ∼2 eV, while the block B3 follows B2 without any gap in the energy.

maxima corresponding to the Au and Te atoms, respectively. Along the long equatorial Au—Te bonds the Au maximum valence electron density is 2.97 e Å^{-3}, situated 0.55 Å away from the Au center, the Te maximum is 0.58 e Å^{-3}, situated 1.05 Å away from the Te center, and the minimum is 0.47 e Å^{-3}, 1.48 Å from the Au atom. Along the short apical Au—Te bond, the Au maximum is 3.25 e Å^{-3}, situated 0.51 Å away from the Au center, the Te maximum is 0.52 e Å^{-3}, situated 0.52 Å away from the Te center and the minimum is 0.27 e Å^{-3}, 1.51 Å from the Au atom. Details of the electron density distribution in the interatomic regions along the chemical bond directions are represented in Fig. 2.

The electronic clouds do not have a spherical symmetry, being polarized towards the neighboring atoms. The polarization is visible for the Au electronic clouds in the 0.28 e Å^{-3} difference between the density maxima values along the two directions and for the Te electronic clouds in the 0.53 Å difference between the maximum density radius along the two directions. The minima of the valence electron density along the equatorial and the apical bond represent 15.8 and 8.18% from the Au maximum, and 81.0 and 51.1% from the Te maximum, respectively. The minima of the valence electron density along the Te—Te bonds are 0.14 and 0.23 e Å^{-3} in the basal (001) and diagonal $(\bar{1}10)$ plane, respectively. They reveal the existence of chemical bonds between the Te atoms, which is in accordance with the tellurium trend to polymerize in three-dimensional networks. However, one must emphasize that this is the *average* structure of the incommensurately modulated structure. The study of the impact of the distortions on the valence-electron density pattern due to the modulations are beyond the purpose of the present paper and will be the object of a further study.

Analysis of the electronic band spectrum and the corresponding density of states (DOS; Fig. 3), in agreement with the study of Krutzen & Inglesfield (1990), reveals the metallic character of the average structure. This is an important characteristic of the charge-density wavesystems, for which the modulation destroys the Fermi surface and opens a band gap (Mitchell & Burdett, 1995).

The same analysis allows us to separate three main blocks of electronic bands. The first block, B1, with a 4.9 eV energy

width is the lowest in energy and contains the first four electronic bands. The second block, B2, follows after a small gap of 1.7 eV and contains the next 12 bands localized over a 3.7 eV energy width, while the third block, B3, follows right after B2, without any energetic gap, containing the rest of the bands with electrons relatively delocalized. There is a certain difficulty in establishing the exact number of bands corresponding to B3 due to the metallic character of the average structure which spreads the 46 valence electrons over more than 23 electronic bands. Further, we may obtain a spatial image of the electron density distribution corresponding to any band or group of bands. This allows us to determine the geometrical characteristics of the electronic bands, such as the localization, how they belong to different atoms and to different orbitals, their degree of hybridization *etc.*, not only for occupied orbitals but also for unoccupied orbitals.

The block B1 contains the energetically lowest four bands with eight electrons, belonging mainly to the Te 5*s* orbitals with a small participation of some *d*-type Au orbitals. They are fully occupied and localized around the Te centers with a slightly deformed spherical local symmetry. Their corresponding distribution, shown in Fig. 4(*a*), has maxima of 0.2438 e Å^{-3}.

The block B2 contains the next 12 electronic bands, also fully occupied. This charge stems mainly from Au 5*d* and less important, from Au 6*s* and Te 5*p* orbitals. The corresponding density, presented in Fig. 4(*b*), is highly localized around the Au atoms with an almost spherical local symmetry with maxima of 2.519 e Å^{-3}. The Te participation generates the existence of some small local charge lobes with densities of the order 0.1075 e Å^{-3}.

Block B3 contains the rest of the electronic bands. This charge stems mainly from the hybridization of Au 6*s* and 5*d* and Te 6*p* orbitals. All the electronic bands within B3 contain components from both Au and Te atoms. Owing to the metallic character of the average structure of calaverite not all of them are fully occupied. We can distinguish a bonding or anti-bonding character according to the amount of electron density distributed along the interatomic directions. Thus, bands 17 (Fig. 5*a*), 18, 19, 20 and 21 (Fig. 5*b*) possess a bonding character, but less pronounced at the 17th band, while bands 22, 23 (Fig. 5*c*), 24 and 25 (Fig. 5*d*) possess an anti-bonding character, more pronounced at the 25th band. The electronic bands possessing a bonding character are the main bands responsible for the chemical bonds between the Au and Te

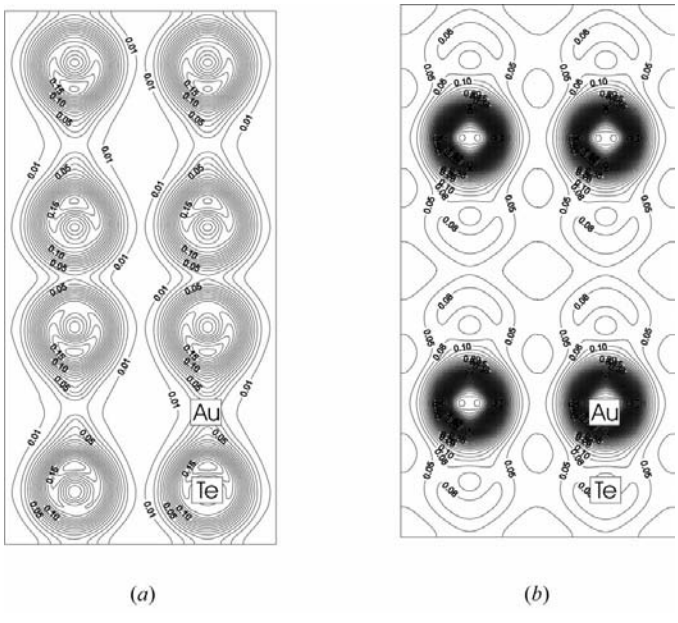

Figure 4
Partial valence electron density corresponding to (*a*) block B1 and (*b*) block B2. In block B1 the maxima correspond to the Te atoms, while in block B2 the maxima of the valence electron density correspond to the Au atoms. Contour lines in intervals of (*a*) 0.01 and (*b*) 0.025 e Å^{-3}.

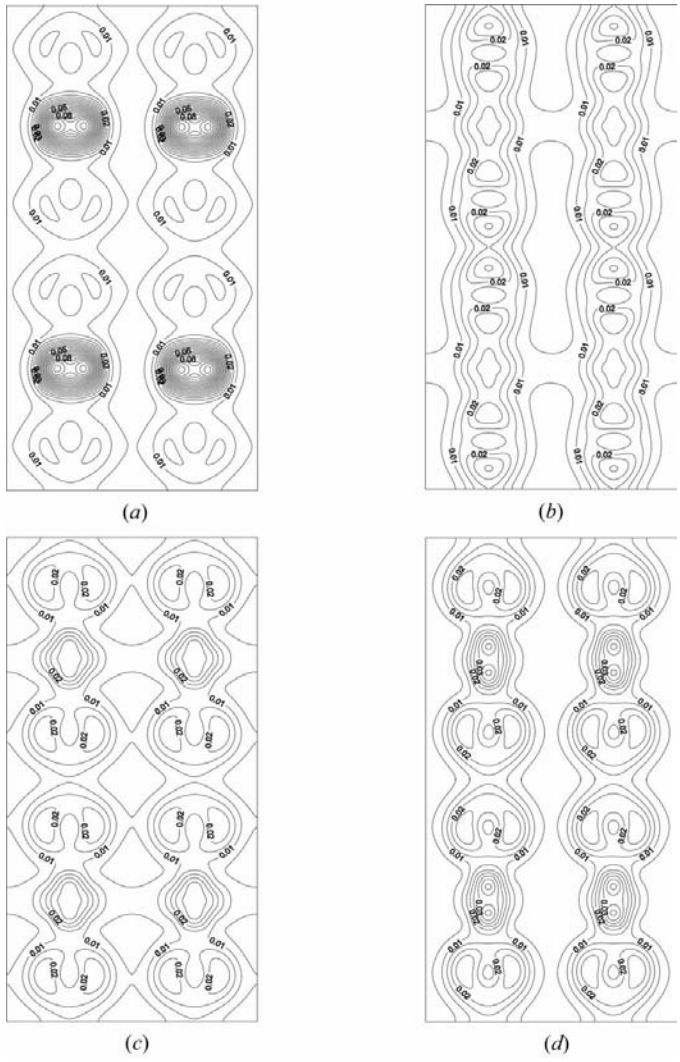

Figure 5
Partial valence electron density corresponding to some selected electronic bands from block B3. (*a*) Band No. 17; (*b*) band No. 21; (*c*) band No. 23; (*d*) band No. 25. Contour lines in the interval 0.005 e Å^{-3}. The position of Au and Te atoms is identical as in Fig. 3.

atoms. The electronic clouds corresponding to these bands are polarized with maxima mainly toward the neighboring atoms.

4. Conclusions

The valence electron density of the average structure of calaverite, calculated using the LDA of DFT, is distributed mainly in the equatorial planes ($\bar{2}01$) of the $AuTe_6$ octahedra interconnected along the apical directions [$\bar{1}01$]. The Te atoms are bonded with each other and with the Au atoms.

The local maxima are located around the Au and Te atoms. The Au maximum valence density is 2.97 and 3.25 e $Å^{-3}$ along the longer and shorter Au—Te bond, respectively. The Te maximum valence electron density is 0.58 and 0.52 e $Å^{-3}$ along the longer and shorter Au—Te bond, respectively.

We can energetically separate three main blocks of electronic bands corresponding, respectively, to

(i) the Te 6*s* orbitals,

(ii) the Au 5*d* orbitals with a secondary hybridization of Au 6*s* and Te 6*p* orbitals, and

(iii) a hybridization of Au 6*s*, 5*d* and Te 6*p* orbitals.

Bands 17–21, belonging to the third block, are responsible for the chemical bonds. The average structure possess metallic character.

The understanding of the electronic properties of the average structure constitutes the basis for the understanding of the incommensurate instability. This will be further analyzed using similar tools.

References

ABINIT (1999). *ABINIT*, Version 2.0. Common Project of the Université Catholique de Louvain, Corning Incorporated and other contributors, http://www.pcpm.ucl.ac.be/abinit.

Causa, M., Dovesi, R., Pisani, C. & Roetti, C. (1986). *Acta Cryst.* B**42**, 247–253.

Charlier, J.-C., Gonze, X. & Michenaud, J.-P. (1991). *Phys. Rev. B*, **43**, 4579–4589.

Dam, B., Janner, A. & Donnay, J. D. H. (1985). *Phys. Rev. Lett.* **55**, 2301–2304.

Goldschmidt, V., Palache, Ch. & Peacock, M. (1931). *Neues Jahrb. Mineral. Geol. Paleontol.* **63**, 1–58.

Gonze, X. (1996). *Phys. Rev. B*, **54**, 4383–4386.

Gonze, X., Caracas, R., Sonnet, Ph., Detraux, F., Ghosez, Ph., Noiret, I. & Schamps J. (2001). Fundamental Physics of Ferroelectrics, AIP Conference Proceedings Vol., 13–20 February, 2000, Aspen, USA.

Hohenberg, P. & Kohn, W. (1964). *Phys. Rev. B*, **136**, 864–871.

Janner, A. & Dam, P. (1989). *Acta Cryst.* A**45**, 115–123.

Kohn, W. & Sham, L. J. (1965). *Phys. Rev. B*, **140**, 1133–1138.

Krutzen, B. C. H. & Inglesfield, J. E. (1990). *J. Phys. Condens. Matter*, **2**, 4829–4847.

Mitchell, J. F. & Burdett, J. K. (1995). *J. Chem. Phys.* **102**, 6762–6777.

Monkhorst, H. J. & Pack, J. D. (1976). *Phys. Rev. B*, **13**, 5188–5192.

Payne, M. C., Teter, M. P., Allan, D. C, Arias, T. A. & Joannopoulos, J. D. (1992). *Rev. Mod. Phys.* **64**, 1045–1097.

Reithmayer, K., Steurer, W., Schulz, H. & de Boer, J. L. (1993). *Acta Cryst.* B**49**, 6–11.

Schutte, W. J. & de Boer, J. L. (1988). *Acta Cryst.* B**44**, 486–494.

Smith, H. (1902). *Mineral. Mag.* **13**, 125.

Triest, A. van, Folkerts, W. & Haas, C. (1990). *J. Phys. Condens. Matter*, **2**, 8733–8740.

Troullier, N. & Martins, J. L. (1992). *Phys. Rev. B*, **43**, 1993–2006.